

## DUOPLASMATRON PARAMETERS FOR OPTIMUM POSITIVE OR NEGATIVE ION YIELD

M. A. ABROYAN, V. P. GOLUBEV, V. L. KOMAROV, G. V. TARVID,  
G. M. TOKAREV AND S. G. TSEPAKIN

*D.V. Efremov Scientific Research Institute of Electrophysical Apparatus, Leningrad, U.S.S.R.*

This paper describes three modifications of a duoplasmatron type ion source. Results of investigation of these sources are given.

The pulsed duoplasmatron makes it possible to obtain a hydrogen ion beam with current up to 2 A. The phase-space density is 600 mA/mrad·cm for 800 mA output current. Proton percentage in the beam is 90 per cent; the heavy ion component does not exceed 2 per cent.

The duoplasmatron for obtaining positive ions of hydrogen provides a beam with current from 2 to 60 mA. In this case one can obtain up to 70 per cent  $H_1^+$ , up to 60 per cent  $H_2^+$ , or up to 70 per cent  $H_3^+$ . A system of diagrams is provided for selection of parameters of the source power supply and the source geometry.

The duoplasmatron for obtaining negative ions gives an  $H_1^-$  ion beam with current up to 150  $\mu$ A. Gas leakage is about 0.7 cm<sup>3</sup>/hour at atmospheric pressure per 1  $\mu$ A current of  $H_1^-$ . Normalized emittance is 0.005 mrad·cm.

The ion beam intensity depends to a great extent on the quality of an ion source. The phase-space volume, mass percentage and beam intensity are essentially determined by the ion source. The beam purity, i.e., the presence of only those ions which are to be accelerated is an important property of the source.

Recently the duoplasmatron type source has gained over-all recognition.<sup>(1)</sup> The duoplasmatron is used in injectors of synchrotrons,<sup>(2,3)</sup> neutron and electrostatic generators,<sup>(4,5)</sup> and in tandem generators.<sup>(6)</sup>

During the past three years the D. V. Efremov Scientific Research Institute has developed a number of duoplasmatron modifications, designed for different accelerators:

1. A pulsed duoplasmatron with  $H_1^+$  ion current up to 2 A.
2. A duoplasmatron with positive hydrogen ion current up to 60 mA.
3. A duoplasmatron with  $H_1^-$  ion current up to 150  $\mu$ A.

The present paper describes the construction of these duoplasmatrons and gives the results of investigations carried out. Current and phase-space characteristics of ion beams and their mass percentage were investigated as a function of the extraction region configuration and the operating conditions of the source.

A general feature of source construction is the

exclusion of organic materials from constructional elements of the gas-discharge chamber. As electric insulation (insulator between anode and intermediate electrode, insulators for cathode leads) metal ceramics with kovar rings brazed to them are used. Vacuum seals are made with annealed copper gaskets. This allows vacuum bakeout of the sources and rapid cleaning of the surfaces of the gas-discharge chamber, i.e., prevents the appearance in the discharge of impurities which can result in generating plasma oscillations<sup>(7)</sup> and cause the beam phase volume to increase.

### 1. PULSED DUOPLASMATRON WITH $H_1^+$ ION CURRENT UP TO 2 A

Obtaining currents of the order of some amperes per pulse is not a problem. The problem is in forming a proton beam with high phase-space density, comprising no heavy ions.

A general view of the duoplasmatron is given in Fig. 1.

A sintered oxide cathode of a cylindrical form is used as the electron emitter. The source coil has 5000 ampere-turns.

In source operation the discharge current of from 50 A to 100 A was maintained by a pulse modulator with a pulse length from 10  $\mu$ sec to 100  $\mu$ sec. At discharge currents of more than 100 A and pulse duration of 100  $\mu$ sec, the voltage drop between the source anode and cathode was observed (Fig. 2).

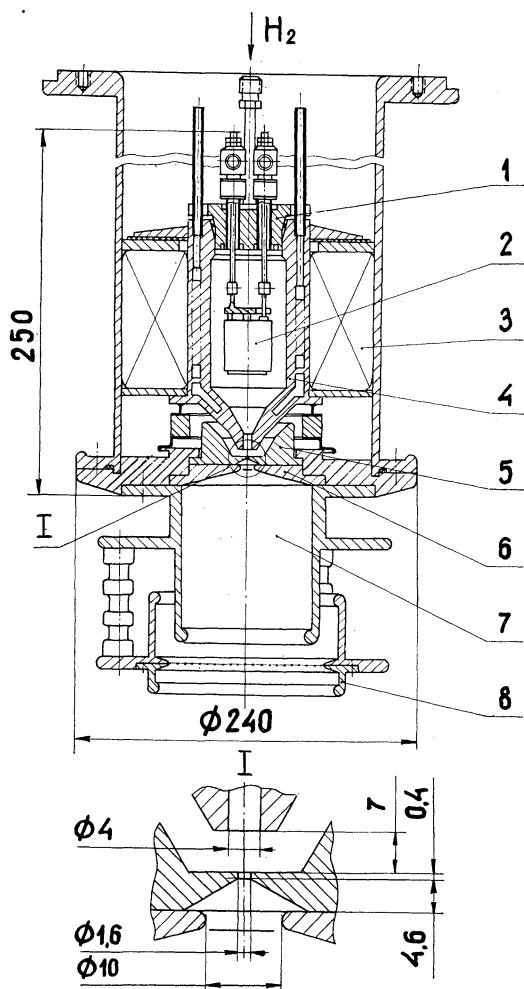


FIG. 1. General view of the pulsed duoplasmatron: 1—stainless-steel cathode block; 2—cathode; 3—electromagnet coil; 4—water-cooled intermediate electrode; 5—copper anode; 6—anode magnet pole; 7—expander; 8—extractor. Dimensions are in millimeters.

This drop is associated with cathode sparking.<sup>(8)</sup> As the pulse duration decreases to 10 to 30  $\mu$ sec the cathode stability to sparking increases. Sparking is an undesirable process, because it leads to cathode destruction and to appearance of oscillations in the discharge. The discharge can be ignited without cathode heating, but such an operation is less stable.

Extraction of ions is accomplished from the developed surface of the plasma, which penetrates into the cylindrical expander. The results, presented in this paper, are obtained with an expander whose depth is 100 mm and whose diameter is

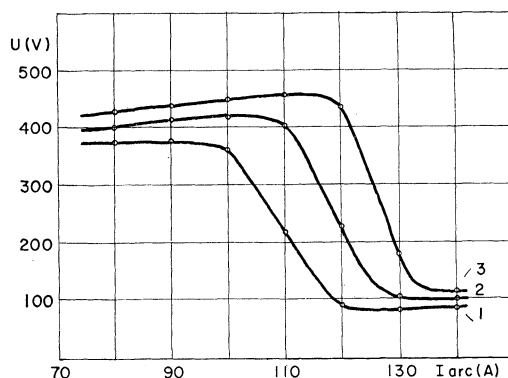


FIG. 2. Discharge current voltage characteristic.  $p = 3.2 \times 10^{-5}$  torr (1);  $4.2 \times 10^{-5}$  (2);  $5.2 \times 10^{-5}$  torr (3); pressure changed with changing the leakage into the source.

75 mm. The hole in the extracting electrode is covered by a grid with 90 per cent transparency.

The ion beam current was measured at a distance of 200 mm from the extracting electrode. Only plasma focusing of the beam was used. The measurements were made by an electric method and checked by calorimetric ones. The collector current in the operating conditions of the source was about 1 A, and in forced operation up to 2 A (Fig. 3).

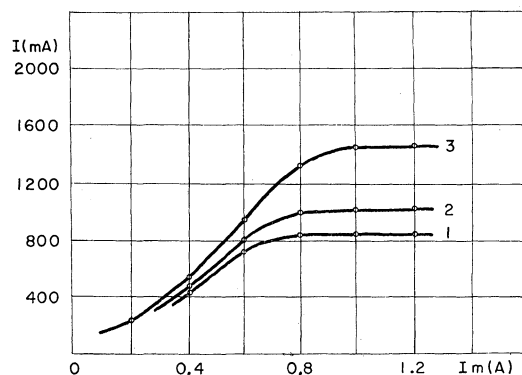


FIG. 3. Beam current  $I$  with changing current in the source electromagnet.  $p = 3.2 \times 10^{-5}$  torr; discharge current  $I_{arc} = 90$  A; extracting voltage  $U = 50$  kV (1); 60 kV (2); 70 kV (3).

Mass-analysis of the beam has shown that the heavy component of the beam ( $M > 3$ ) does not exceed 1 to 2 per cent; the proton component of the beam is from 85 per cent up to 90 per cent of total current.

The source phase-space characteristics were

measured by the method of diaphragming the beam, then registered on film and photometered. This method is a particular case of the four-slit method and provides more complete information about the phase-space characteristics of the beam, i.e., the phase-space density distribution in the four-dimensional phase-space volume.<sup>(9)</sup> The normalized two-dimensional phase-space area  $V$  was defined from the four-dimensional volume  $V_{inv}$ , calculated from the measurement results with the help of the expression

$$V = (2V_{inv})^{1/2}. \quad (1)$$

The mean phase-space density, defined as

$$j = \frac{I}{V}$$

was 600 mA/mrad·cm at a current of 800 mA. Figure 4 shows the phase-space diagram of the ion beam for a beam current of 1.32 A and an energy of 50 keV.

When decreasing the pulse duration from 100 μsec to 30 μsec a phase-space density increase to 750 mA/mrad·cm was observed. The lifetime of

the source in continuous operation is defined by the cathode lifetime and is not less than 200 hours.

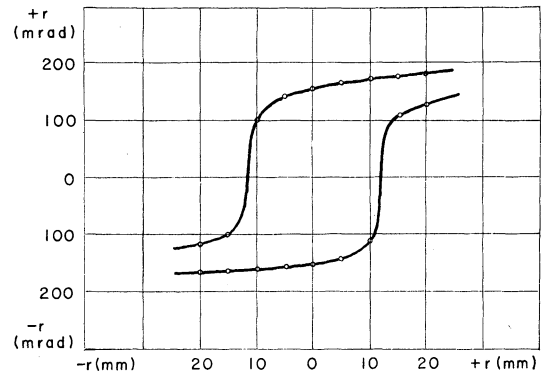


FIG. 4. Phase-space diagram of the beam. The beam current—1.32 A, the energy—50 keV.

## 2. DUOPLASMATRON WITH POSITIVE HYDROGEN ION CURRENT UP TO 60 mA

The main difficulty in the development of this duoplasmatron was to provide the required ion

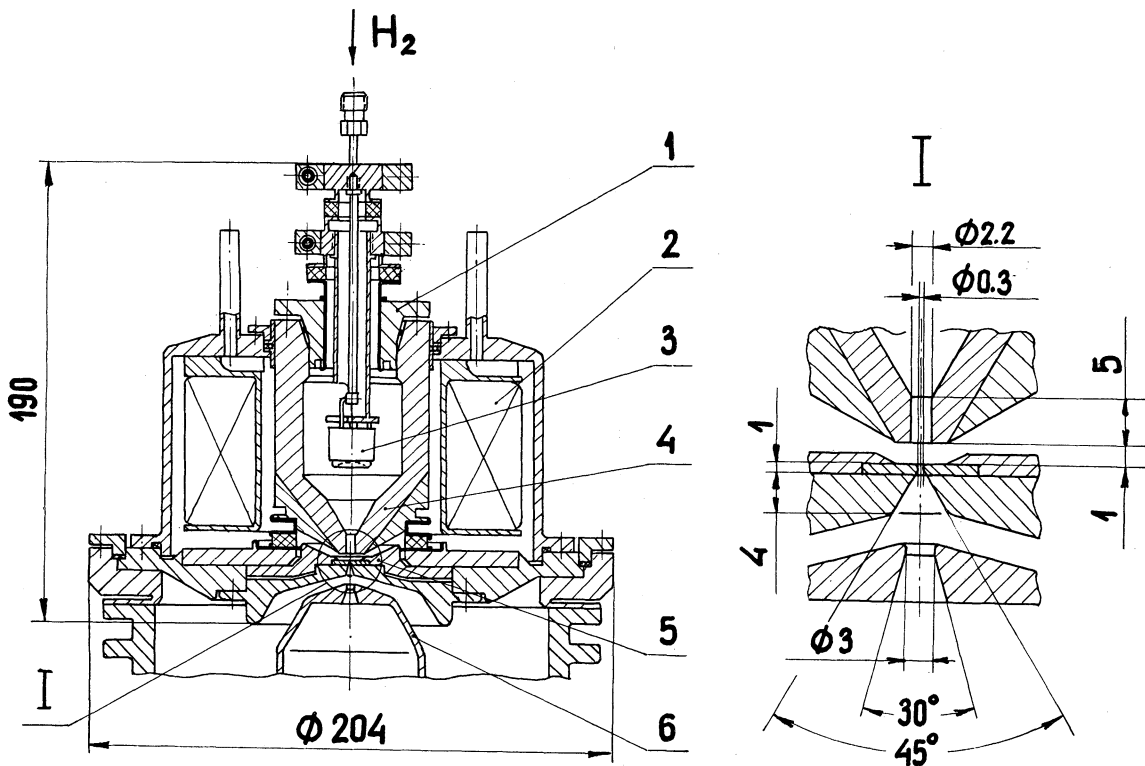


FIG. 5. General view and extraction region of the duoplasmatron ions for current up to 60 mA. 1—cathode block; 2—electromagnet coil; 3—cathode; 4—intermediate electrode; 5—anode insert; 6—extractor. Dimensions are in millimeters.

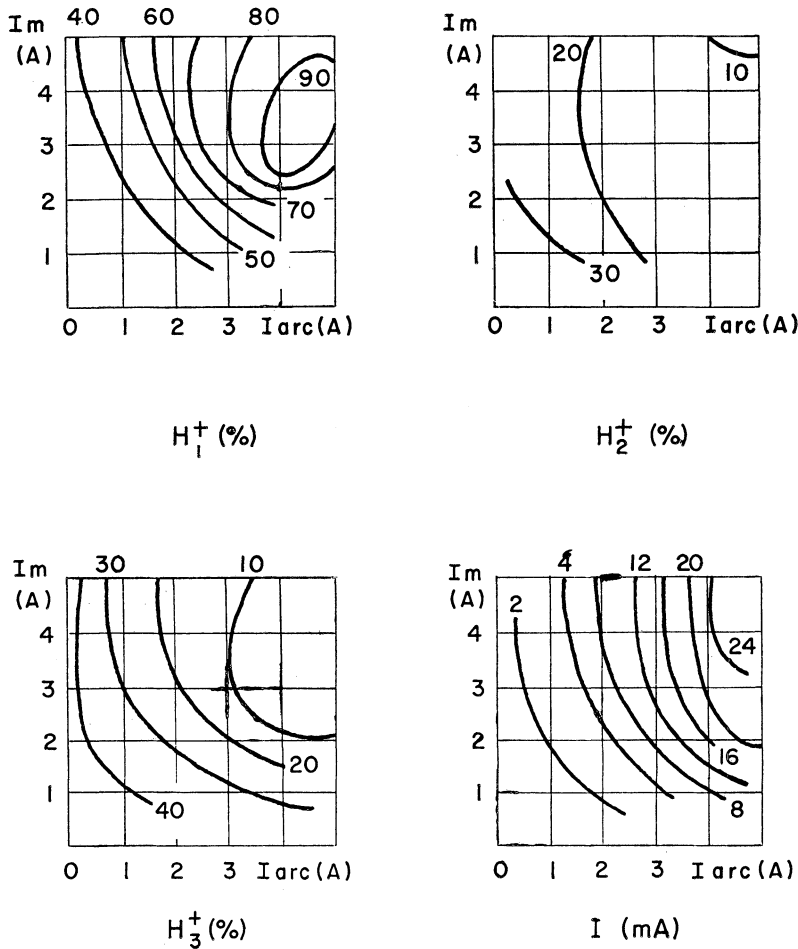


FIG. 6. Percentage of hydrogen ions ( $H_1^+$ ,  $H_2^+$ ,  $H_3^+$ ) and beam current  $I$  as a function of the discharge current  $I_{arc}$  and the coil source current.

mass percentage of the beam at high economy of the source.

The general view of the source is given in Fig. 5.

In this source an impregnated tungsten-barium cathode with a spherical emitter is used. The cathode lifetime is not less than 300 hours in operation with oil-vapor pumps.

The source is designed for a discharge current of 5 A. The source coil has 3000 ampere-turns.

The anode consists of two anode inserts: a copper insert with a pressed-in infusible gasket and a magnetically-soft-material one. Heat removal is accomplished by anode cooling.

Dependence of the beam current value and component percentage on the gas-discharge region configuration, emission channel geometry and discharge parameters were investigated in detail.

For defining the characteristics of the source the

dependence diagrams of the beam current and component percentage on the discharge parameters were plotted. Such diagrams for a definite geometry of the anode region at a constant pressure in the gas-discharge chamber are shown in Fig. 6.

The beam parameters were investigated for variation of the emission hole from 0.3 to 0.6 mm and for distances between the intermediate electrode and anode from 0.8 mm to 7 mm. The system of diagrams obtained, similar to that of Fig. 6, permits selection of parameters of the power supply and the source geometry depending on the accelerator parameters and application. The nature of the curves in these diagrams also permits the definition of some manufacturing defects of each source, for example, noncoaxiality or low quality manufacture of the anode gasket.

From the source ion beam currents from 2 mA

to 60 mA can be obtained. If the discharge parameters and the anode-intermediate electrode spacing are properly selected one can obtain ion beams comprising either no less than 70 per cent  $H_1^+$  or no less than 60 per cent  $H_2^+$ , or no less than 70 per cent  $H_3^+$ .

As an example the source parameters for a neutron generator are given in Table I.

TABLE I

Beam current	5 mA
Discharge current	no more than 3 A
Proton component	75 per cent
Gas consumption	no more than 8 cm <sup>3</sup> /hour at atmospheric pressure
Normalized emittance	0.144 mrad · cm
Discharge voltage	110 V
Source coil	3000 ampere-turns
Cathode heater power	no more than 100 W
Source intake power	no more than 480 W
Emission hole diameter	0.3 mm

The phase-space diagram of the hydrogen ion beam is shown in Fig. 7. With this source it is possible to obtain beams of He, Ar, Xe, Kr, or N ions with currents of 3 to 5 mA.

The continuous operation lifetime of the source is limited by destruction of the infusible anode

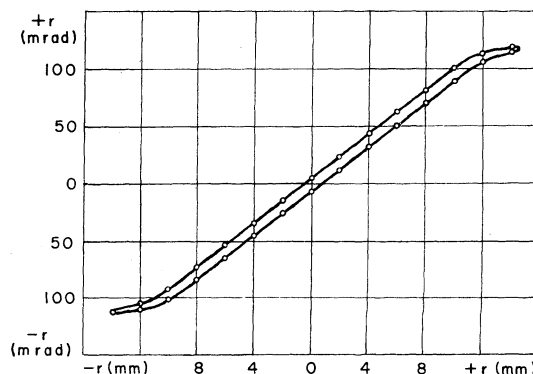


FIG. 7. Phase-space diagram of the hydrogen ion beam. Beam current 10 mA; energy 30 keV.

gasket and is not less than 150 hours (in the operating conditions given in Table I).

### 3. DUOPLASMATRON WITH $H_1^-$ ION CURRENT UP TO 150 $\mu$ A

In this source the principle of extraction of hydrogen ions from the periphery of the plasma column, compressed by magnetic field and existing in a neutral gas medium, is used. This principle is described in Refs. (6, 10, 11).

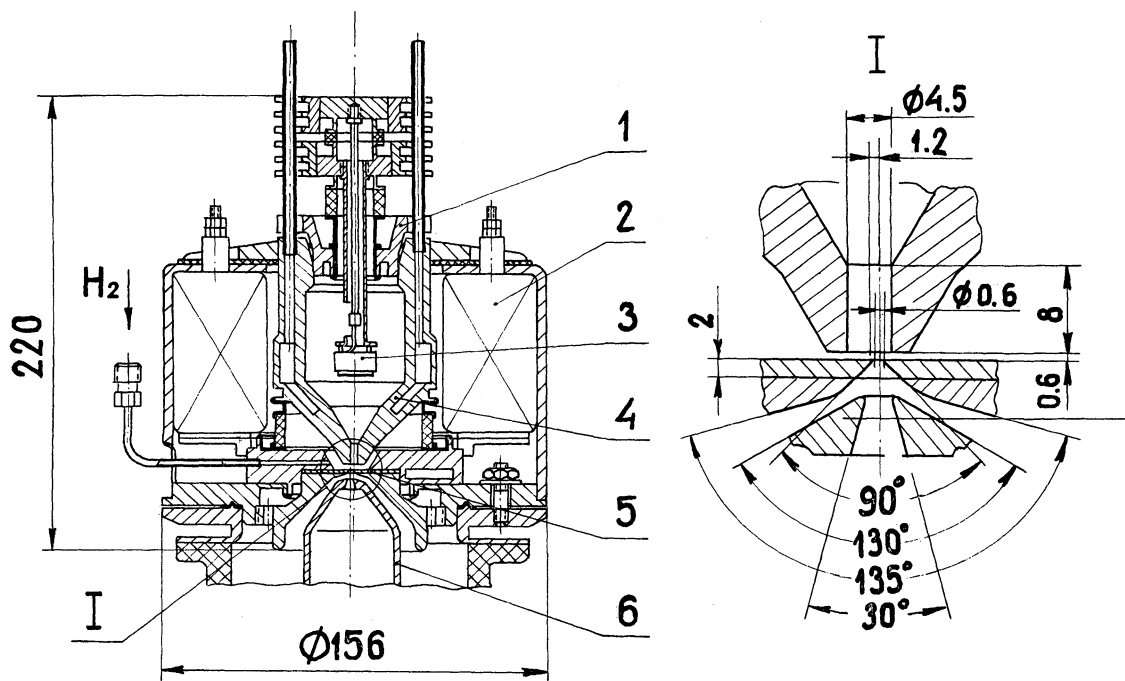


FIG. 8. General view and extraction region of the duoplasmatron ions for obtaining  $H_1^-$ . 1—cathode block; 2—electromagnet coil; 3—cathode; 4—intermediate electrodes; 5—anode insert; 6—extracting electrode. Dimensions are in millimeters.

The general view of the source is illustrated in Fig. 8.

The anode hole is displaced relative to the channel axis in the intermediate electrode.

Gas injection is in the region between the anode and intermediate electrode. It is shown experimentally that yield of negative ions increases considerably compared to gas injection from the cathode block side. In the source an impregnated tungsten-barium cathode is used. The cathode lifetime is no less than 500 hours in operation with mercury-vapor pumps; the intake power is 80 W. The cathode block is air-cooled.

Figure 9 shows the beam current of negative ions and electrons, accompanying the ion beam, as a function of the source coil (1500 turns) current.

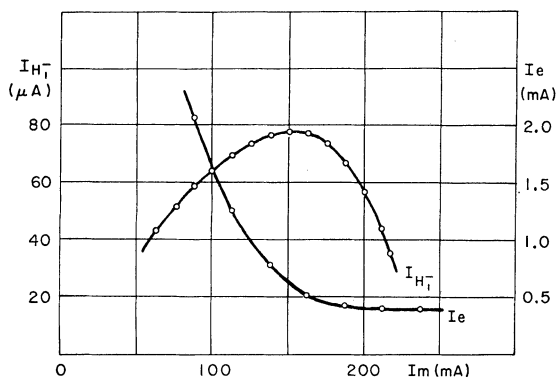


FIG. 9. Ion beam current and electron current with changing the coil source current.  $I_{\text{arc}} = 3 \text{ A}$ ;  $\text{H}_2$  leakage =  $50 \text{ cm}^3/\text{hour}$  at atmospheric pressure.

When the direction of this current is changed, the values of ion and electron currents on the source output are changed by 20 to 30 per cent. This seems to be explained by the focusing action of the inhomogeneous magnetic field in the anode hole region. In addition, as a result of the displacement of the channel axis of the intermediate electrode, the magnetic field is distorted. This leads to the fact that the axes of the electron and ion beams do not coincide, and the angle between them is of a few degrees.

Figure 10 shows the phase-space diagram of the ion beam. The diagram is plotted from the measurements, made after a lens by the two-slit method.

With the ion source described it is possible to obtain beams of  $\text{H}_1^-$  ions with current up to  $150 \mu\text{A}$  for currents of accompanying electrons of no more than 500 mA and for gas leakage of about  $0.7 \text{ cm}^3/\text{hour}$  at atmospheric pressure, per  $1 \mu\text{A}$  of  $\text{H}_1^-$  ions.

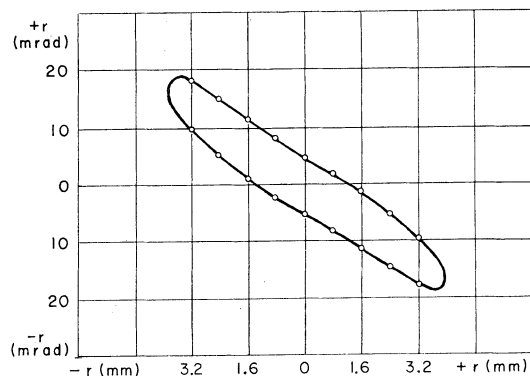


FIG. 10. Phase-space diagram of the  $\text{H}_1^-$  ion beam. The energy is 20 keV.

The normalized emittance value of the obtained beam does not exceed  $0.005 \text{ mrad} \cdot \text{cm}$ . The mean phase density is about  $30 \text{ mA/mrad} \cdot \text{cm}$ .

The continuous operation lifetime of the ion source is defined by the cathode lifetime. The lifetime of the anode inserts which are made of tungsten and tantalum is not less than 1000 hours at arc discharge currents of 1 to 2 A.

## CONCLUSION

As a consequence of these investigations the operating conditions and construction of ion sources were optimized. Application of metal-ceramic joints allowed us to minimize the number of disjunctions and to improve substantially the quality of operation and the stability of the sources.

## ACKNOWLEDGEMENT

The authors wish to express their gratitude to Z. G. Solnyshkova for investigation and preparation of electron emitters.

## REFERENCES

1. M. von Ardenne, 'Tabellen der Elektronenphysik, Ionenphysik und Übermikroskopie', *VEB Deutscher Verlag der Wissenschaften*, **B1**, 544 (1956).
2. M. A. Abroyan *et al.*, *Trudy Mezhdunarodnoi Konferentsii po Uskoritelam, Dubna, 1963*, p. 507 (Atomizdat, Moscow, 1964).
3. B. Vošicki, M. Buzić, and A. Cheretakis, *Proc. Linear Accelerator Conference, Los Alamos, 1966*, p. 344 (LA-3609).
4. Yu. B. Evdokimov *et al.*, *Nauchno-tehnicheskaya Konferentsia po Apparature dlia Aktivatsionnogo Analiza, Budapesht*, p. 149 (Atomizdat, Moscow, 1969).

5. C. D. Moak, H. E. Banta, J. N. Thurston, J. W. Johnson, and R. F. King, *Rev. Sci. Instr.*, **30**, 694 (1959).
6. G. P. Lawrence, R. K. Beauchamp, and J. L. McKibben, *Nucl. Instr. Methods*, **32**, 357 (1965).
7. J. Kistemaker, P. K. Rol, and J. Politiek, *Nucl. Instr. Methods*, **38**, 1 (1965).
8. L. N. Vagin, *Zh. Tekh. Fiz.*, **38**, vyp. 8, 1347 (1968).
9. N. F. Ivanov, Yu. P. Sivkov, and A. I. Solnyshkov, *Sb. Elektro-tehnicheskaya Apparatura*, vyp. 4, 3-20 (Atomizdat, Moscow, 1966).
10. A. V. Almazov, Yu. M. Khirnyi, and L. P. Kochemasova, *Pribory i Tekhnika Eksperimenta*, **6**, 36 (1966).
11. K. Bethe and G. Rau, *Nucl. Instr. Methods*, **39**, 157 (1966).

Received 6 August 1970